Collapse Mechanism Analysis in the Design of Superstructure Vehicle

M K Mohd Nor[*1]

Crashworthiness and Collision Research Group, Engineering Mechanics Department, Faculty of Mechanical and Manufacturing Engineering, Universiti Tun Hussein Onn Malaysia, 86400 Parit Raja, Batu Pahat, Johor, Malaysia

E-mail: khir@uthm.edu.my

Abstract. The EU directive 2001/85/EC is an official European text which describes the specifications for "single deck class II and III vehicles" required to be approved by the regulation UN/ECE no.66 (R66). To prevent the catastrophic consequences by occupant during an accident, the Malaysian government has reinforced the same regulation upon superstructure construction. This paper discusses collapse mechanism analysis of a superstructure vehicle using a Crash D nonlinear analysis computer program based on this regulation. The analysis starts by hand calculation to define the required energy absorption by the chosen structure. Simple calculations were then performed to define the weakest collapse mechanism after undesirable collapse modes are eliminated. There are few factors highlighted in this work to pass the regulation. Using the selected cross section, Crash D simulation showed a good result. Generally, the deformation is linearly correlates to the energy absorption for the structure with low stiffness. Failure of critical members such as vertical lower side wall must be avoided to sustain safety of the passenger compartment and prevent from severe and fatal injuries to the trapped occupant.

1. Introduction

Directive 2001/85/EC is the directive of European Parliament and of the council which concerning the special provisions for vehicles used for the carriage of passengers comprising more than eight seats [1]. The legislation helps to design the structure by considering the residual space, components attached to the structure and so on. The survival space can be defined as the remaining space around the passengers during and after a crash. The legislation also describes different tests that can be performed to ensure the deformation not advance beyond the limit of the survival space. This therefore helps to design of the vehicle structure.

Failure of the side and roof vehicle structures to sustain the passenger safety compartment can cause fatal accidents to the occupant inside the vehicle [2]. Statistics related to rollover impact from all around the word excluding Europe shows 11% accident rate before year of 2001, 38% from 2001 to 2003 and 49% from 2004 to 2006 [2]. In Malaysia, vehicle crashes involving lorries and buses is 22.4% and 7.9% from the total accident, from 2007 to 2010 respectively [3]. 11.1% of bus accident is caused by the factor of superstructure under rollover with highest percentage of fatalities occurrence (60%) [4]. International standard related to protection of passenger in rollover accidents are commonly applied on new vehicles and regulated for design approval. Malaysia is one of 58 countries that follow Regulation No. 66 of the Economic Commission for Europe of the United Nations (UN/ECE) -

Uniform Provisions Concerning the Approval of Large Passenger Vehicles with Regard to the Strength of Their Superstructure (R66) as standard vehicle approved [4]. This regulation provides an option of certification based on full-scale vehicle testing (physical prototype test), or by numerical simulation (digital prototype test) [5]. The rollover test approach normally involves the lateral tilting test by locating a simplified vehicle on the tilting platform, with blocked suspension [6]. This approach has been adopted to investigate rollover characteristics of heavy vehicle rollover using ANSYS simulation tool referring to R66 [2]. Review to rollover statistic before 1990 from 1988, its account for about 70% of the heavy vehicle occupant fatalities, while the injury and harm distribution in rollovers by body region state the highest percentage of brain and head [7]. From 1991 to 2000, the number of passenger vehicles involved in fatal crashes rises by 4% [8]. Rollover crashes follow a very similar pattern to other crashes, with a rise in the number of involved vehicles beginning in 1994 and increasing through 1999. In 2004, there were an estimated 393,545 occupants in passenger vehicles that rolled over, as compared to 415,418 occupants in 2000, a 5.3% increase [9].

Failing to preserve survival space for passenger and driver by roof intrusion is a fatality risk that could lead to death. Beside the amount of roof intrusion to protective structure, occupant also can be ejected from the vehicle by its moment of inertia. While observing to injury outcomes, the injuries on the body after a rollover had taken place were concerned on the head, chest and arms. 42.5 % of the belted occupants (non-ejection) in vehicle accidents resulting in a rollover were injured in the head, 26.2 % on the chest and 44.6 % of the arm [10]. It can be concluded the design of superstructure plays an important role to avoid fatal accident due to the collapse of survival space. Therefore, in this work, Crash D simulation tool that is designed to analyse collapse mechanism of structural frameworks is used to predict and design the desired collapse mechanism of a superstructure vehicle based on EU directive 2001/85/EC.

2. Analysis Description

Crash D is a nonlinear matrix analysis computer program designed for the collapse analysis of structural frameworks. The program can allow for both material and geometric sources of nonlinearity and some features are tailored to deal with problems peculiar to vehicle structures. Crash D is based on the matrix analysis (or finite element) approach where the structure is considered as an assemblage of a finite number of individual beams connected at a finite number of nodal points (nodes). Nodes can be assumed anywhere in the structure, but they are usually associated with points where beams are joined together, where elastic or collapse properties of a continuous beam are changed, where loads are applied or where supports are attached, etc.

Position of each node is determined by 3 Cartesian coordinates corresponding to an arbitrarily but conveniently chosen global coordinate system x, y and z. This system is common to all nodes. This allows for simplified analysis compared to the initial geometry of the structure, defined by node coordinates in the global system and by the distribution of beams as shown in sections 3 and 4. The Crash D analysis uses the individual stiffness matrices to assembly the general stiffness matrix of the complete structure. This general matrix combined with restraints specified at the supports, then represents a mathematical model of the real structure in its initial state before loading is applied.

It can be seen in the following section that the external loads are applied to the selected nodes as concentrated forces. It also can be moment and/or displacements. Each node then has 6 displacement components (3 translations along and 3 rotations about the global axes x, y and z). The analysis then returns to each individual beam and calculates the displacements vector to produce the beam end-loads after the first increment of the external loads. The end loads of each individual beams are compared with the specified collapse criteria - this is shown in Section 8. Whenever the local loads exceed the maximum strength the appropriate mode of collapse is simulated by changing the boundary conditions at the collapsed beam end. If no collapse is detected, the local boundary conditions remain unchanged. The same sequence of events is repeated after each increment, until either the maximum specified load/displacement/energy absorbed is reached, or until the structure starts collapsing, making it

impossible to increment load any further. By incrementing displacement rather than loads one can analyse the structural behaviour even after it starts collapsing.

2.1. Finite Element Modelling for Collapse Analysis

Careful definition of the exact aims of the analysis is absolutely essential prior to any structural modelling. This is particularly true for the selection of loading cases and of the criteria to judge the safety performance of a structure. Safety criteria as shown in this paper usually involve prediction of the maximum strength and/or energy absorbing capacity and/or remaining strength (in rollover or falling object protective structures) and /or force or acceleration history during impact and/or maximum deformations. It is very important to realize that stiffness, maximum strength and energy absorbing capacity of a structure are different properties, not necessarily proportional to each other. It is also important to note that the Crash D analysis performed in this paper cannot predict the dynamic fluctuating forces or accelerations during impact. The analysis can cope, however with the structural deformation and energy absorption problems in those structures where dynamic and quasi static collapse modes are similar.

2.2. Idealisation of the Actual Structure

This section justifies the assumption made in this paper regarding the idealization of the actual structure under consideration.

Collapse analysis must predict the correct overall collapse mechanism of the complete structure, i.e. correct location hinges. Therefore, to perform the analysis of superstructure in this paper, nodes are placed in all locations where hinges may occur as defined in Section 4 using collapse mechanism analysis since the Crash D analysis can identify hinges at nodal points only. It can be observed in the following section that energy absorption and collapse mechanism analysis have been adopted to define the possible hinges area within the structure. Assuming uniform strength components hinges can be seen occur at the points of maximum bending moments.

The collapse model may sometimes include only a part of complete structure which will envelop the correct collapse mechanism. The relevant segment may be extracted using previous experience as adopted in this paper, or the result of preliminary elastic calculation of the complete structure. Preliminary elastic analysis of the complete structure may be necessary in more complex cases in order to identify the main load paths and to estimate the effect on the load distribution of components which are not included in the collapse model. Other modelling tricks such as using dummy-beams may be employed to simulate various effects of the parts of the structure which are not included in the collapse mode, but a detailed discussion of these exceeds the limits of this paper.

3. Energy Calculation

The document 2001/ 85/EC proposes method to get the total energy that has to be absorbed by the structure during testing as shown below:

$$E^* = 0.75Mg\left[\sqrt{\left(\frac{W}{2}\right)^2 + {H_s}^2} - \frac{W}{2H}\sqrt{H^2 - 0.8^2} + 0.8\frac{H_s}{H}\right] \text{ (Nm)} \quad (1)$$

where M, g, W, H_s, and H refer to the unladen mass of the vehicle, gravitational acceleration ($9.81ms^{-1}$), the overall width, the height of the centre of gravity of the unladen vehicle and the height of the vehicle respectively.

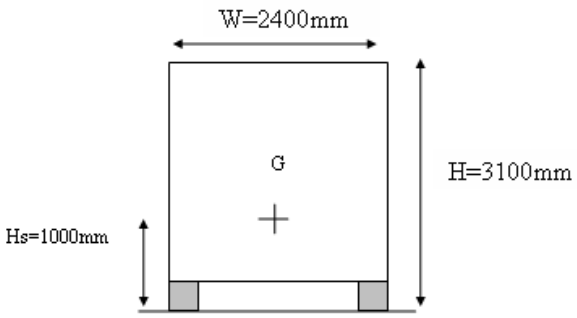

Figure 1. Specification of Superstructure Geometry

Using the definition in [11] where a superstructure vehicle such as large tractor has an unladen weight in excess of 7250kg, a superstructure with 9000 kg mass is considered in this analysis as shown in figure 1. Using the geometry values in this figure into equation (1), the total energy absorbed by the whole structure is obtained as:

$$E^* = 0.75x9000x9.81\left[\sqrt{\left(\frac{2.4}{2}\right)^2 + 1^2} - \frac{2.4}{2x3.1}x\sqrt{3.1^2 - 0.8^2} + 0.8\frac{1}{3.1}\right] \quad (2)$$

Thus it can be calculated the total energy that has to be absorbed by the superstructure is 43.7 kNm

4. Analysis of Collapse Mechanism

In the event of crash and impact, most of the energy is absorbed by plastic deformation of vehicles. The structures of vehicle are collapse in bending mode of the beams. The initial failure and deep collapse will experience by the weakest collapse mechanism that is depends on the mode of collapse. In any structures, there are several possible collapse mechanisms. The structure under consideration has 3 redundancies hence collapse will take place whenever 4 plastic hinges formed.

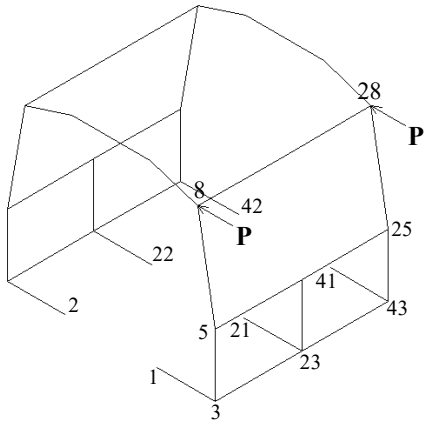

Figure 2. Effective loads during rollover

Based on the discussion in Section 2.2, the superstructure is modelled using 48 beams and 46 nodes as shown in figure 2 where load is applied at nodes 8 and 28. To choose the right collapse mechanism, the factor of residual space must be considered first. It is, therefore, a rotation mechanism of the floor is neglected to protect the area of occupant's legs, the seats and others related components attached within the floor. In addition, the design structure should have a capability to give the lowest possible

force experienced by occupant. Hence, the synchronization between forces and plastic moment must be established. In order to give the lowest force experienced by occupant, collapse mechanisms that give the largest angle rotation of the structure must be identified before it reach and touch the residual space.

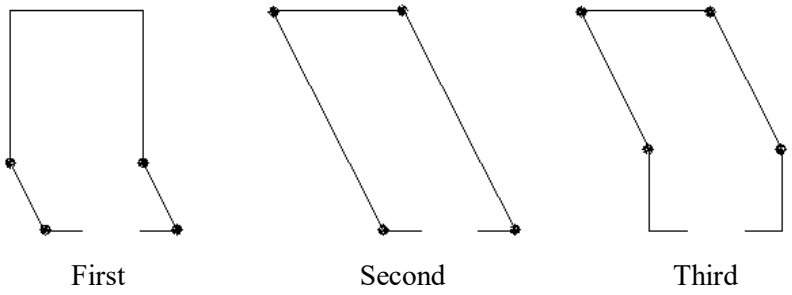

Figure 3. Three possible collapse mechanisms

To ensure the lowest force experienced by occupant, collapse mechanism that give the largest angle rotation of the structure before it reach and touch the residual space must be chosen. Then, plastic moment can be calculated using energy balance method. The remaining possible collapse mechanisms when load is applied at nodes 8 and 28 is shown below:

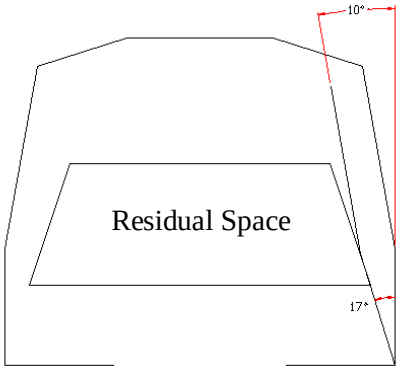

Figure 4. Maximum rotation of the First Collapse Mechanism

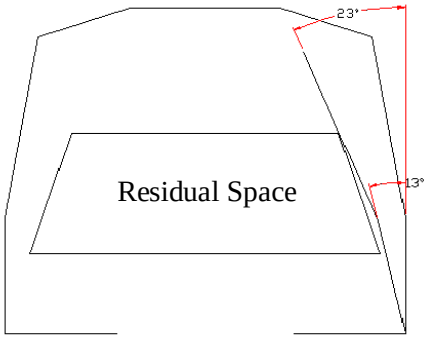

Figure 5. Maximum rotation of the Second Collapse Mechanism

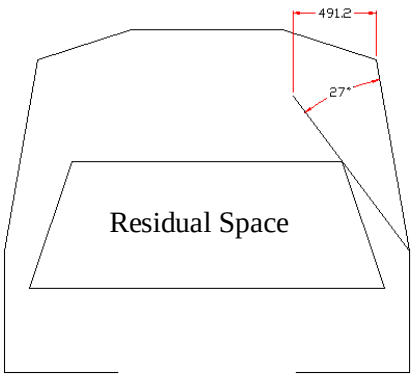

Figure 6. Maximum rotation of the Third Collapse Mechanism

Referring to figures 4 to 6, it can be concluded that the third collapse mechanism is the mode that can give the lowest force to our occupant as it gives the highest rotation angle (27º). This statement can be clarified by calculating plastic moment M_p for each collapse mechanism. The corresponding energy absorbed by one ring can be obtained by dividing the energy of the whole structure with 7. Using the value of energy in equation (2):

$$E_{ring} = \frac{E_{structure}}{7} = 6250.8\ J \tag{3}$$

Subsequently, the strain energy in one ring due to plastic deformation is used to get equation (4) to get the plastic moment M_p formulation:

$$E_{deformation} = 4\theta M_p \tag{4}$$

Table 1. Plastic Moment M_p for each collapse mechanism

Collapse Mechanism	Plastic Moment, M_p
1st	5266.7 Nm
2nd	4984.7 Nm
3rd	3317.8 Nm

Table 1 summarizes the value of plastic moment for each collapse mechanism. The analysis performed in this section show a good agreement with the previous conclusion. As can be observed, third collapse mechanism experiences the lowest value of M_p compared to the other collapse mechanisms. Therefore, the structure will collapse in this mechanism since it is the weakest collapse mode. The value of M_p then can be used to define a suitable tube properties of the superstructure's cross section.

5. Analysis of Cross Section Properties

As mentioned in the preceding section, most of the structure is likely to deform in bending mode. Nevertheless, both bending and torsion properties must be considered to run Crash D. For bending properties, M_p is identical in respect to y and z axes since the cross section is symmetrical about these axes. Further the tube can be divided into two identical sections to simplify the analysis.

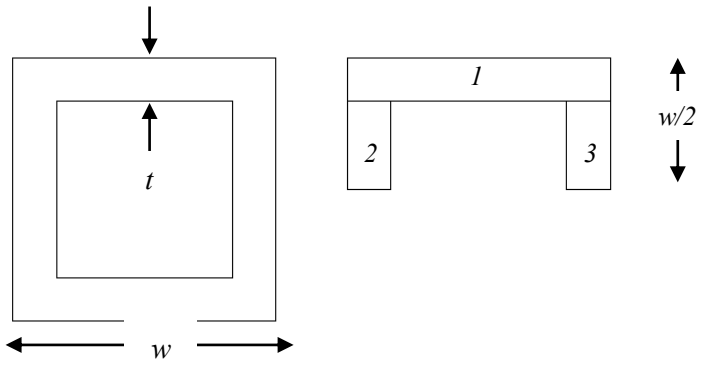

Figure 7. Cross section properties of the tube

Figure 7 shows cross section properties of the tube under consideration. Plastic moment M_p of this cross section can be calculated as follows:

$$M_p = \sum(F_i \text{ x } D_i) \text{ x } 2 = \sum(\sigma_y \text{ x } A_i \text{ x } D_i) \text{ x } 2 \quad (5)$$

where σ_y, D_i and A_i refer to yield stress, distance from origin and area of each section respectively. As shown in figure 7, the cross section is divided into 3 major sections hence section 2 is identical to section 3. Substituting A_i and D_i of each section into equation (5), M_p can be rewritten as:

$$M_p = 2 \text{ x } \sigma_y \text{ x } \left(\frac{3}{4} \cdot w^2 \cdot t - \frac{3}{2} \cdot w \cdot t^2 + t^3\right) \quad (6)$$

The value of plastic moment M_p for each cross section within the superstructure then can be calculated using this equation.

6. Static Analysis

Regarding collapse mechanism, only the window pillar and roof members are allowed to collapse. Therefore, the longitudinal limb must be chosen to transfer load from window pillars to the middle side wall. Detail static analysis can be performed to determine the stiffness of each section to be further used in Crash D. It is expected that the stiffness of window pillar and roof members is lower than the vertical lower sidewall and the floor member, hence been used as a primary reference to start up the analysis. Static analysis allows for the actual structure condition examination for the case load is applied at node 8. The calculated ratio then can be used to manipulate the stiffness of other members to get the desired collapse mechanism. This eventually helps the most suitable cross section identification using Crash D simulation.

It should be noted the analysis that has been performed is defined for 2D structure, therefore, must be modified for 3D structure. First the equilibrium equations must be obtained. According to the requirements, points 1 and 8 must be completely restrained.

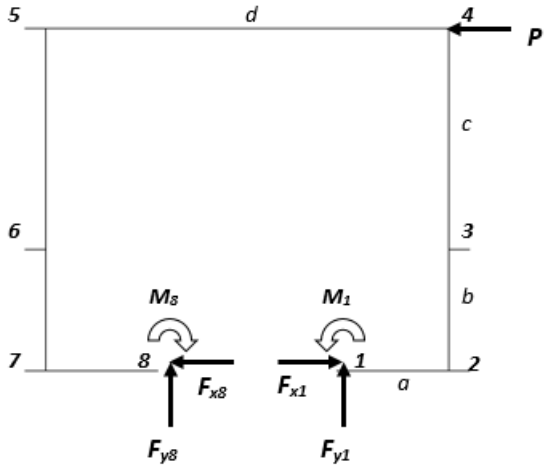

Figure 8. Simplified 2D structure

Both moment and load is applied about x and y directions to these points as shown in figure 8. There are 3 redundancies obtained when the equilibrium equations are applied hence require 3 compatibility conditions to solve all unknowns. Further bending moment is defined for each member 1-2, 2-3, 3-4, 4-5, 5-6, 6-7 and 7-8. The energy contributed by axial forces is neglected as the structure is assumed collapse mainly due to bending mode. The derived bending equations then can be integrated with an energy equation by assuming all cross sections are identical.

Table 2. Reactions at points 1 and 8

M_1	M_8	F_{x1}	F_{x8}	F_{y1}	F_{y8}
$-1225\mathrm{P}$	$-775\mathrm{P}$	$-\mathrm{P}/2$	$-\mathrm{P}/2$	$0.453\mathrm{P}$	$-0.453\mathrm{P}$

Applying the compatibility conditions into the energy equation, the value of each support reactions is summarized in table 2. The bending moment distributions along 2D structure can be further calculated for each member by using moment equation defined previously.

Table 3. Bending moment for each points

Point 1	Point 2	Point 3	Point 4	Point 5	Point 6	Point 7	Point 8
$775\mathrm{P}$	$472\mathrm{P}$	$112\mathrm{P}$	$-543\mathrm{P}$	$543\mathrm{P}$	$112\mathrm{P}$	$-472P$	$-775\mathrm{P}$

The value of each point is given in table 3. It can be observed that the weakest collapse mechanism is not similar to the one defined previously. The points of plastic hinges obtained in this analysis are 1, 4, 5 and 8. This is not acceptable since the floor will rotate. Therefore, the stiffness of the members must be modified by manipulating the cross section.

Ratio of bending moment between the longitudinal members at point 3 and the lower side wall with the floor at points 1 and 2 is calculated respectively. The ration between the floor and the longitudinal members is calculated as 775P/112P. The ratio between the lower side wall and the longitudinal members is calculated as 472P/112P. The value is adopted to choose the most appropriate cross section of the superstructure.

6.1. Tube Cross-Section Selection

To run Crash D simulation, the stiffness ratio between the floor, lower side wall and the roof should be revised from 2D to 3D framework. For that purpose, ratio of bending moment is used to define stiffness of the superstructure members:

$$\frac{3 \cdot I_{floor}}{2 \cdot I_{roof}} = 6.92 \quad \frac{3 \cdot I_{lower\ side\ wall}}{2 \cdot I_{roof}} = 4.21$$
$$= 4.61 \qquad = 2.81 \tag{7}$$

To choose the reference roof stiffness using energy balance equation, the value of plastic moment defined from collapse mechanism is subtracted with the value of plastic moment for each cross section. The second moment of area for cross section with the closest value then is used as a reference roof stiffness. Generally, the ratio calculated in equation (7) can be used directly to define floor and lower side wall stiffness. However, it is preferable to increase the value a little bit higher since the longitudinal member is known as the point where load is transferred. It should be stiffer than the roof because low stiffness can affect collapse behaviour of the whole structure. Therefore, referring to the value of ratio defined in equation (7), 5 and 3 are used for the floor and lower side wall respectively. The identical stiffness for roof, window pillar and longitudinal members then can be used.

Table 4. Properties of the chosen cross sections

Member	W (mm)	t (mm)	A (mm^2)	M_p (Nmm)	I (mm^4)	T_p (Nmm)	J (mm^4)
Floor	100	3	1164	$1.06x10^7$	$1.83x10^6$	$7.5x10^6$	$3.00x10^6$
Lower Side wall	80	4	1216	$8.67x10^6$	$1.17x10^6$	$6.4x10^6$	$2.04x10^6$
Longitudinal	60	3	684	$3.66x10^6$	$3.71x10^5$	$2.7x10^6$	$6.48x10^6$
Roof and Window Pillar	60	3	684	$3.66x10^6$	$3.71x10^5$	$2.7x10^6$	$6.48x10^6$

The related values of the chosen cross section for Crash D simulation are finally determined is summarized in table 4.

6.2. Moment-Rotation Response

To determine moment-rotation response for each section, a simple cantilever beam with force applied at the end of the beam to develop bending effect can be adopted.

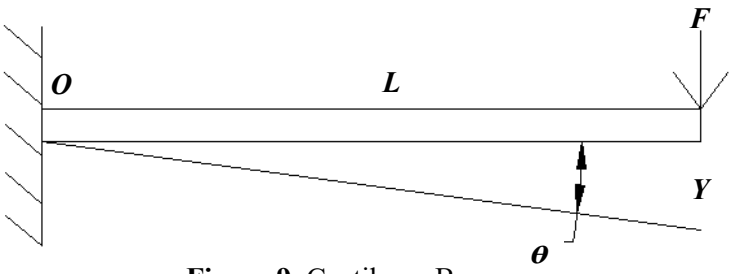

Figure 9. Cantilever Beam

Figure 9 shows the cantilever beam. It can be observed that the maximum bending response created at point *O*. Differentiating strain energy of the beam, the deflection *Y* and moment-rotation response *M(ɵ)* can be determined.

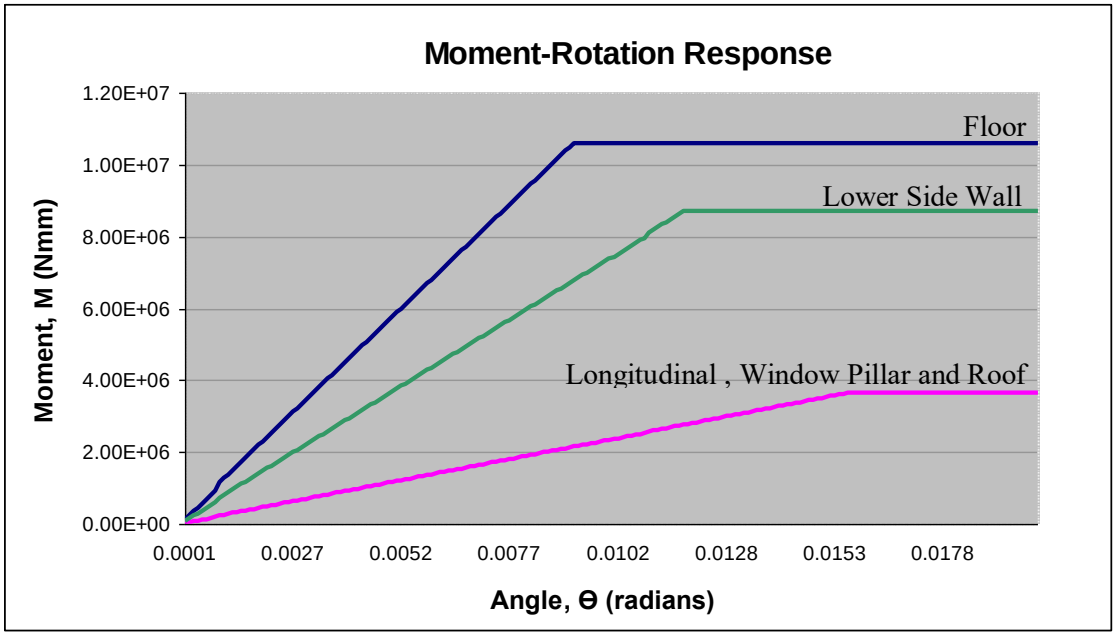

Figure 10. Moment vs. Rotation Angle Diagram

Diagram in figure 10 then can be plotted. It shows moment-rotation response for the selected cross section for each member. (E = 208 000MPa, L = 1000mm)

7. Input Data for Crash D

The analysis preformed in the preceding section is used to select the most appropriate geometry of cross section for each superstructure members to achieve the desired collapse mechanism. There are few other parameters has to be defined correctly before the simulation can be conducted.

Referring to the chosen collapse mechanism shown in figure 6, the displacement is 491.2 mm. This value can be used as a maximum horizontal displacement of nodes 8 and 28 before the structure collapse and hit the survival area.

The right boundary conditions must be applied to run Crash D analysis correctly. In this analysis, a rigid body motion within the structure is undesirable. Therefore, nodes 1, 2, 21, 22, 41 and 42 have to be fully constrained to avoid any movement. In addition, rotation in x and y directions is set to zero (0) as each joint is assumed rigid.

The identical cross section is defined for roof and window pillars. Finally, the simulation is run for hundred (100) times cycles. Complete Crash D input file data for this analysis is given in appendix A.

8. Crash D Simulation-Results and Discussions

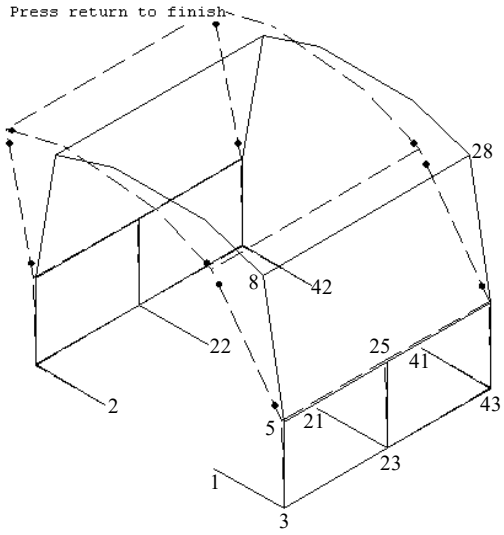

Figure 11. Plastic hinges in the superstructure

Figure 11 shows plastic hinges that occur within window pillars and the roof. It can be observed that the Crash D simulation predicts the same collapse mechanism as mentioned in the preceding section.

Concerning the results, first plastic hinges occurred within cycle 8 at both nodes 8 and 28 (roof) along elements 5, 8, 8, 10 and elements 25, 28, 28, 30 respectively. During the cycle, the deformation energy is only $4.72\text{Ex}10^5$ Nmm and the horizontal displacement is 39.3 mm. The next plastic hinges observed in the window pillar (node 5 and 25) within cycle 11. The corresponding energy increased significantly to almost 83 percents as compared to the previous plastic hinges while the horizontal displacement is also increased to 54 mm.

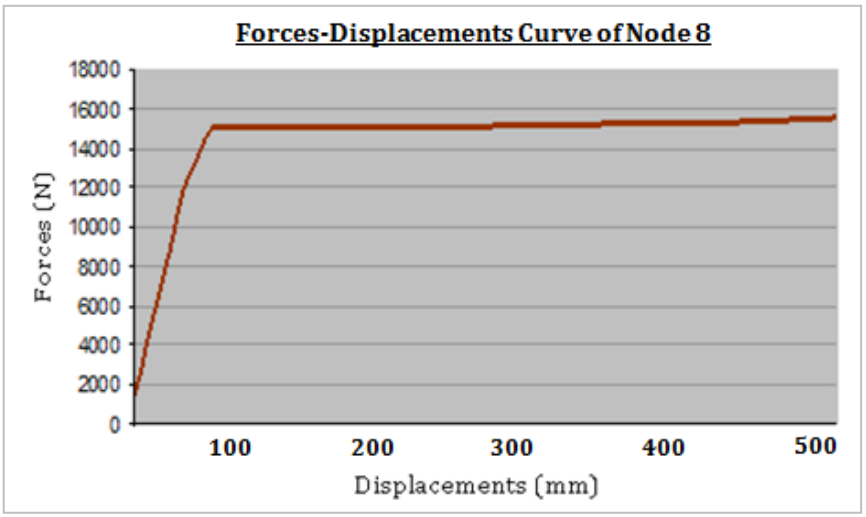

Figure 12. Forces vs. Displacement of node 8

During the final cycle (100), the total energy absorbed by the whole superstructure is calculated as $1.4122\text{x}10^7$ Nmm. The difference is about 11.2% compared to the energy absorbed calculated in the beginning of this analysis. The difference is expected due to the limitation to choose the right cross

section. Basically the right method has been adopted in this analysis using an energy balance to calculate M_p. However, the value cannot been used directly since there are only few available cross sections for selection to find the closest value of M_p.

Generally, for the structure with low stiffness, the deformation correlates linearly to the energy absorbed. The same energy value cannot be obtained from Crash D results. This requires interpolation between cycles 89 and 90 to give 15381.95 N force and 438.8 mm deflection at node 8. Even though it is just a small deflection, it is still capable of producing high force experienced by the occupant.

Figure 12 shows the diagram of force vs. displacement values of node 8. Referring to this figure, as expected, the trend can be divided into two: elastic and plastic parts. In respect to plastic part, two different behaviours are observable. The force is constant as the plastic hinges starts to develop then increase due to the subsequent increment of loads.

In respect to the design structure, stiffness (strength), energy absorption (deformation) and collapse mechanism has to be considered in the analysis. The structure can be designed to have a very high stiffness to avoid large deformation; however, it will lead to a large force experienced by the occupant in the event of crash and impact. Contrarily, if the structure is too weak, it can easily penetrate the survival area. Hence, the analysis must compromise and consider these factors wisely.

The Crash D simulation results show that few members contribute to sustain the load within the desired collapse mechanism. Window pillars and longitudinal members connected to the roof basically have no value of yield ratio. In addition, the longitudinal members connected to the floor have a low yield ratio. Therefore, the cross section of these members can be reduced optionally perhaps to reduce weight of the vehicle structure. In the other hand, few members such as vertical lower side wall (nodes 3, 5 and nodes 23, 25) is very important to sustain load during impact since it has the highest yield ratio as compared to the other members. Their cross section therefore cannot be modified to a smaller size.

9. Conclusion

In this paper, collapse mechanism analysis in the design of superstructure vehicle is reviewed. Few factors are highlighted to pass the regulation UN/ECE no.66 (R66). The chosen approach is thoroughly conducted to avoid penetration and damage within the occupant area. The weakest collapse mechanism is identified after the other undesirable collapse modes are eliminated. Using the selected geometry and simulation setting (input data), good results are provided by Crash D simulation, and agree with the selected collapse mechanism.

10. References

[1] Official Journal of European Communities (2001), Directive 2001/85/EC of the European Parliament and of the Council of 20 November 2001 relating to special provisions for vehicles used for the carriage of passengers comprising more than eight seats in addition to the driver's seat, and amending Directives 70/156/EEC and 97/27/ECSinha, S. and Ghosh, S. (2006), "Modeling cyclic ratcheting based fatigue life of HSLA steels using crystal plasticity FEM simulations and experiments", *International Journal of Fatigue*, vol. 28, no. 12, pp. 1690-1704

[2] M. K. Mohd Nor, M. Z. Dol Baharin, Rollover Analysis of Heavy Vehicle Bus, Applied Mechanics and Materials, Vol. 660 (2014), pp 633-636

[3] Z. A. A. Noor, M. F. S. Atiqah, L. Fauziana, and A. M. Abdul Rahmat, MIROS crash investigation and reconstruction annual statistical report f–2011, Tech. Rep. MRR 05/2012, Malaysian Institute of Road Safety Research, Kuala Lumpur, Malaysia, 2012Furnish, M. D. and Chhabildas, L. C. (1998), "Alumina strength degradation in the elastic regime", *AIP Conference Proceedings,* vol. 429, no. 1, pp. 501-504

[4] MIROS, UNECE WP 29 Regulation Implementation in Malaysia: An Update Malaysia with

UNECE Regulation Implementation, vol. 25, no. June, pp. 23–26, 2009
[5] United Nation, "Regulation No 66 of the Economic Commission for Europe of the United Nations (UN/ECE) — Uniform provisions concerning the approval of large passenger vehicles with regard to the strength of their superstructure Incorporating," no. 66, pp. 1–45, 2011.
[6] A. Strashny, An Analysis of Motor Vehicle Rollover Crashes and Injury Outcomes, DOT HS 810 741, Washington, DC, 2007
[7] K. H. Digges, "Summary Report of Rollover Crashes," 1990
[8] W. Deutermann, *Characteristics of Fatal Rollover Crashes*, no. April. Mathematical Analysis Division, National Center for Statistics and Analysis National Highway Traffic Safety Administration, U.S. Department of Transportation, 2002, pp. 1–54.
[9] A. Strashny, "An Analysis of Motor Vehicle Rollover Crashes and Injury Outcomes," 2007.
[10] D. O. Christian Krettek, "Rollover Accidents Of Cars In The German Road Traffic : An In-Depth Analysis Of Injury And Deformation Pattern," pp. 1–12, 1998.
[11] Department of Transport, Leaflet No 1, Guidelines on Maximum Weight and Dimensions of Mechanically Propelled Vehicles and Trailer, 2015

Acknowledgments
The author wishes to convey a sincere gratitude to Universiti Tun Hussein Onn Malaysia (UTHM) and Ministry of Higher Education Malaysia (MOHE) for providing the financial means during the preparation to complete this work under Fundamental Research Grant Scheme (FRGS), Vot 1547.

Appendix A. Crash D Input File

```
ECE Reg. 66  ROLL-OVER CAGE STRUCTURE A    UPRIGHT  1 INTERMEDIATE PILLAR
NODES
1    530 0    0
2   -530 0    0
3   1200 0    0
4  -1200 0    0
5   1200 720  0
6  -1200 720  0
8   1000 1850 0
9  -1000 1850 0
10   450 2030 0
11  -450 2030 0
21   530 0    2000
22  -530 0    2000
23  1200 0    2000
24 -1200 0    2000
25  1200 720  2000
26 -1200 720  2000
28  1000 1850 2000
29 -1000 1850 2000
30   450 2030 2000
31  -450 2030 2000
41   530 0    1000
42  -530 0    1000
43  1200 0    1000
44 -1200 0    1000
45  1200 720  1000
46 -1200 720  1000
BEAMS
1  1  3  4 1 1 10 180 1                    Floor
```

```
3  2  4  4 1 1 11 180 1                    Floor
5  3  5  4 1 2 4  180 12          Sidewall
6  4  6  4 1 2 3  0   12Sidewall
7  5  8  4 1 3 6  180 2           Sidewall
8  6  9  4 1 3 5  0   2           Sidewall
9  8  10 4 1 3 2  180 2                    Roof
10 9  11 4 1 3 1  0   2           Roof
11 10 11 4 1 3 1  0   2                    Roof
21 21 23 4 1 1 30 180 1                    Floor - Ring 2
23 22 24 4 1 1 31 180 1                    Floor     "
25 23 25 4 1 2 24 180 12        Sidewall  "
26 24 26 4 1 2 23 0   12          Sidewall  "
27 25 28 4 1 3 26 180 2                    Sidewall  "
28 26 29 4 1 3 25 0   2                    Sidewall  "
29 28 30 4 1 3 22 180 2                    Roof      "
30 29 31 4 1 3 21 0   2                    Roof           "
31 30 31 4 1 3 21 0   2                    Roof      "
35 41 43 4 1 1 45 180 1                    Floor - Intermediate
36 42 44 4 1 1 46 180 1                    Floor         "
37 43 45 4 1 2 44 180 12        Sidewall - Stump-Pillar
38 44 46 4 1 2 43 0   12          Sidewall      "
39 5  45 4 1 1 43 180 11        Waist Rail
40 25 45 4 1 1 43 180 11        Waist Rail
41 6  46 4 1 1 44 180 11        Waist Rail
42 26 46 4 1 1 44 180 11        Waist Rail
43 8  28 4 1 1 43 180 11        Cant Rail
44 9  29 4 1 1 44 180 11        Cant Rail
45 3  43 4 1 1 41 180 11        Floor Rail
46 23 43 4 1 1 41 180 11        Floor Rail
47 4  44 4 1 1 42 180 11        Floor Rail
48 24 44 4 1 1 42 180 11        Floor Rail
MATERIAL
1 208000 0.3
ELPROP
1 1164 3.000E06 1.83E06  1.83E06 Elastic Property 1
2 1216 2.048E06 1.17E06  1.17E06 Elastic Property 2
3 684  6.48E05  3.71E05  3.71E05 Elastic Property 3
HINGPROP
1  3 7.50E06  1.06E07 1.06E07 7.50E06  1.06E07 1.06E07      Floor Plastic Property
2  3 2.70E06  3.66E06 3.66E06 2.70E06  3.66E06 3.66E06      Window Pillar Plastic Property
11 3 2.70E06  3.66E06 3.66E06 2.70E06  3.66E06 3.66E06      Longitudinal Members Plastic Property
12 3 6.40E06  8.67E06 8.67E06 6.40E06  8.67E06 8.67E06      Lower Sidewall Pillars Plastic Property
CYCLES
2 5E7 100 0 8 1 1 0  Loadis, Enemax, Number of Cycles etc. (see CRASHD Manual)
LOADS
8  -491.2 0 0 0 0 0            Cant Rail Impact Prescribed Deflection
28 -491.2 0 0 0 0 0            Cant Rail Impact Prescribed Deflection
RESTR
1  1 1 1 1 1 1                 Centre Floor Restraint
2  1 1 1 1 1 1                 Centre Floor Restraint
3  0 0 1 1 1 0
4  0 0 1 1 1 0
5  0 0 1 1 1 0
6  0 0 1 1 1 0
8  1 0 1 1 1 0                 X Restraint indicates Prescribed Deflection on Node 8
9  0 0 1 1 1 0
```

```
10 0 0 1 1 1 0
11 0 0 1 1 1 0
21 1 1 1 1 1 1          Centre Floor Restraint
22 1 1 1 1 1 1          Centre Floor Restraint
23 0 0 1 1 1 0
24 0 0 1 1 1 0
25 0 0 1 1 1 0
26 0 0 1 1 1 0
28 1 0 1 1 1 0          X Restraint indicates Prescribed Deflection on Node 28
29 0 0 1 1 1 0
30 0 0 1 1 1 0
31 0 0 1 1 1 0
41 1 1 1 1 1 1          Centre Floor Restraint
42 1 1 1 1 1 1          Centre Floor Restraint
OUTPUT
1 2 1 2 1 1 1 1 1
END
```